Journal of JSCE, Vol. 2, 144-158, 2014

THE EFFECT OF LOG PILING ON LIQUEFACTION

Saima RIAZ[1], Atsunori NUMATA[2], Kaori MIMURA[3], Hiroaki IKEDA[4] and Toshikazu HORI[5]

[1]Student Member of JSCE, Department of Civil Engineering, Waseda University
(3-4-1, Okubo, Shinjuku-ku, Tokyo 169-8555, Japan)
E-mail: saimariaz04@gmail.com
[2]Member of JSCE, Chief Research Engineer, Research Institute of Technology, Tobishima Corporation
(5472, Kimagase, Noda-shi, Chiba, 270-0222, Japan)
E-mail: atsunori_numata@tobishima.co.jp
[3]Member of JSCE, Junior Engineer, Engineering Department, Kanematsu-NNK Corporation
(3-2 Kojimachi, Chiyoda-ku, Tokyo, 102-0083, Japan)
E-mail: k-mimura@knn.co.jp
[4]Member of JSCE, Engineer, Showa Material Corporation
(2-45, Kita 20 Chome Hondoori, Shiroisi-ku, Sapporo city, Hokkaido)
E-mail: ikeda@showamaterial.co.jp
[5]Laboratory Chief, Department of Geotechnical & Hydraulic Engineering, National Institute of Rural Engineering
(2-1-6 Kannondai, Tsukuba-shi, Ibaraki 305-8609, Japan)
E-mail: thori@affrc.go.jp

This paper introduces a liquefaction mitigation method that uses log piles as environmentally friendly and practical solution for strengthening civil engineering structures. The liquefaction mitigation measure explored in this paper can be used to increase the earthquake resistance of loose sands by improving the density of soil. During the Tohoku Pacific earthquake in 2011, liquefaction was pervasive in large portions of the region, especially in Tokyo Bay and the city of Urayasu. Extensive liquefaction caused extensive damage to residential properties, electricity, water, sewage networks, and bridges. The mitigation of global warming is an important issue that requires immediate attention. Because the use of wood can be effective for preventing global warming, the authors have considered it to mitigate liquefaction damage. A series of large-scale shaking table tests was performed to investigate the effect of liquefaction mitigation by log piling into sandy ground. The results indicate that the method of log piling is an effective liquefaction mitigation compared with methods for increasing density, such as the densification method. Portable dynamic cone penetration (PDCP), Swedish weight sounding (SWS), automatic ram sounding (ARS), piezo drive cone (PDC), and flat dilatometer (FDM) tests, as well as field tests, were performed in the city of Urayasu. These tests were performed to confirm the effectiveness of log piling on liquefaction mitigation.

Key Words: *liquefaction, shaking table, global warming, log piles, sounding*

1. INTRODUCTION

In 2011, an earthquake occurred along the Pacific coast of the Tohoku and Kanto regions of Japan. The earthquake caused extensive damage to life, property and nuclear power plants due to a tsunami and intensive earthquake motion. Although Tokyo is located approximately 380 km from the epicenter, the ground motions detected during the earthquake were strong enough to cause significant liquefaction to loose reclaimed soils in Tokyo Bay and the city of Urayasu[1)-4)]. Many residential and commercial buildings and lifeline facilities in Urayasu experienced extensive damage due to soil liquefaction.

Soil liquefaction caused severe damage to foundations, lifelines, and waterfront structures. Excessive settlement and lateral spreading of the ground and landslides were induced by liquefaction. Many studies on soil liquefaction have been performed to understand the mechanism of liquefaction and the dynamic responses of foundations in a liquefiable soil[5)-11)]. The results of these studies provided the basis for the evaluation of mitigation methods for liquefaction hazards[12)-16)].

Yasuda and Ogasawara[17] evaluated a countermeasure for liquefaction that involved the installation of steel pipes, which they determined to be effective against liquefaction. Numata et al.[18] analyzed wooden piles as a remedial measure against liquefaction using the 1964 Niigata earthquake as an example. They considered a countermeasure that involved driving wooden piles into the ground, which they determined to be effective against ground liquefaction. They discussed the durability of wood and misunderstandings concerning the utilization of wood as a structural element in the field of civil engineering. They determined that wood could be used as a countermeasure against liquefaction.

Yoshida et al.[19] conducted an experimental study of a liquefaction countermeasure using log piling for residential houses. Small-scale shaking table tests in a 1-g gravity field were performed using a model ground. They discovered that wooden piles could increase the resistance of the ground to liquefaction by increasing the ground density by piling and the dissipation of excess pore water pressure along the surfaces of the piles. As a result, the magnitude of the settlement of the house, which was set on the improved ground with piling logs, was minimized.

Global warming is a significant issue in this century, for which all persons should be responsible. It is primarily caused by the indiscriminate deforestation and production of carbon dioxide by burning fossil fuels. Wood is instrumental in climate change because trees absorb carbon dioxide from the atmosphere as they grow. Therefore, the expansion of forests is a completely natural way to offset global warming. The amount of carbon dioxide that trees absorb from the atmosphere would increase if wood was harvested and used as material for improving foundations instead of steel and concrete, which require a substantially greater amount of fossil fuels and produce carbon dioxide during manufacturing[20)-24)].

Currently, Japan is a forest-rich country; therefore, a vast amount of wood could be harvested. Because the use of wood is effective for mitigating global warming, the authors have considered it as a mitigation measure for liquefaction damage. Logs are rarely used in structural foundations. However, during the construction of the Niigata station in 1958, logs were piled into the ground to construct the foundation. As a result, no damage occurred during the 1964 Niigata earthquake in Japan[25]; however, a building next to the station, which had a concrete pile foundation, incurred some structural damage. Piled logs continue to support the existing Niigata station; these logs may not decay. These findings are evidence that wooden piles can be used as a liquefaction countermeasure.

Wooden piles have been used to remedy liquefaction; this environmentally friendly and economical technique is important, specifically, for developing countries, such as Pakistan, where cost and economic considerations are critical.

Liquefaction-induced flow caused significant damage to structures during previous earthquakes, such as the 1964 Niigata earthquake, the 1983 Nihonkai-chubu earthquake, and the 2011 Tohoku Pacific earthquake in Japan. Studies on liquefaction began immediately after the Niigata earthquake. However, the 1995 Hyogoken-nambu earthquake and the 2011 Tohoku earthquake accelerated these studies due to significant damage to buildings, roads, and bridges. After the occurrence of these earthquakes, many studies based on shaking table tests and analyses were performed.

Several predictions and countermeasures have been proposed and introduced in several design codes. The developed countermeasures have been applied to existing structures. Among these countermeasures, the installation of log piles as structural members is a relatively new countermeasure that is effective against liquefaction. The effectiveness of this method was demonstrated by conducting shaking table tests in the laboratory and in the field. The main objectives of the study are as follows:

1. To examine the liquefaction behavior of the improved foundation using wooden piles.
2. To obtain a cost-effective, practical, and environmentally friendly solution for liquefaction mitigation.
3. To reveal the effect of log piling on liquefaction.
4. To increase the resistance of the ground to liquefaction by increasing ground density and confining pressure.
5. To compare the effects of the densification method and the log piling method on liquefaction.

2. THE SHAKING TABLE TEST

(1) Experimental setup

A series of large-scale shaking table tests was conducted in a 1-g gravity field to evaluate and demonstrate this technique for liquefiable sand during an earthquake. The model ground was set up in a rigid steel container 3,600 mm long, 5,700 mm wide, and 1,800 mm high. The container was divided into two parts; each part had a width of 2,300 mm with a 1,100 mm cavity between each part (as shown in **Fig. 2**). The loose liquefiable model ground was composed of Kasumigaura sand with a relative density of approximately 48%. The model ground was prepared using two methods: the densification method and the log piling method.

To evaluate structural damage caused by liquefaction, a load of concrete with a mass of 1.1 t (prototype contact pressure of 1.1 t/m^2) was placed on the ground surface, which was assumed equivalent to a 2-level wooden house.

Logs with diameters of 8 cm and lengths of 100 cm were used. Piles were driven by statically pushing them into the model ground with an oil jack. The tree species of the logs was Japanese cedar.

Kishida, et al.[26] performed 1-g and centrifuge tests and revealed that the scale of the model ground did not affect the relationship between the log length and the thickness of the liquefaction layer, and the relationship between the settlement of the improved ground and the settlement of the unimproved ground. Large-, medium- and small-scale shaking table tests were conducted in this study. The tests did not yield differing results, which indicate that the scale of the model ground does not affect the settlement results obtained from the shaking table tests.

(2) Case studies

Four cases (NIP, P5D, P4D, and DNS) were examined in the large-scale shaking table test. The symbol NIP denotes no improvement; P5D denotes log piling with an interval of five times the diameter of the pile; P4D denotes log piling with an interval of four times the diameter of the pile and DNS denotes the densification method.

The large-scale shaking table tests are summarized in **Table 1**. Two cases were simultaneously tested on the same shaking table, and the rigid container was divided into two parts as shown in **Fig. 2**. NIP and P5D were tested in container No. 1 and P4D and DNS were tested in container No. 2.

For densification of the model ground, a vibrator was used to compact the soil in layers. The ground water table was set to GL-0.1 m; the surface soil thickness of 0.1 m was a nonliquefaction layer. A bag of coarse cloth filled with crushed stones was placed on the head of each log as a drain.

(3) Sand sample

Samples of Kasumigaura sand were collected (density of soil particles ρ_s = 2.695 g/cm^3, maximum void ratio e_{max}= 1.067, minimum void ratio e_{min} = 0.656, 50% grain size D_{50} = 0.35 mm, and uniformity coefficient U_c = 2.0). The physical properties of the sand and grain size distribution curve are shown in **Fig. 1**. Kasumigaura sand contains almost no fine fraction and is a nonplastic material.

(4) Container and arrangement of sensors

Fig. 2 shows the arrangement and placement of sensors. Accelerometers, pore water pressure gauges and displacement gauges were installed at different locations in the container.

An accelerometer (A00x, A00y, A00z, A01x–A04x, A05x, A05y, A05z, A06x–A09x, A10x, A10y, A10z), a pore water pressure gauge (P0–P12) and a displacement gauge (D1–D8) were used. In addition, the accelerometer (A06x–A09x) and pore water pressure gauge (P07, P08, P11, P12) served as embedded sensors in each log, whereas the remaining accelerometers and pore water pressure gauges were buried in the ground. Sensors A00y, A05y, and A10y were set in the y-axis direction and A00z, A05z, and A10z were set in the z-axis direction. The remaining accelerometers were set in the x-axis direction. The pore water pressure gauges were installed horizontally in the ground. Accelerometer A00 was installed directly on the container. Laser sensors were mounted on a frame above the weight, and targets were fixed on the weight that was placed on the ground surface to measure the vertical displacement of the weight.

Table 1 Case studies.

Cases	Method	Container No.
NIP	No improvement D_r = 48%, D_c = 92.8%	1
P5D	Log piling, Interval = 5D a_s = 3.1%, D_r = 64% D_{ro} = 49%, D_c = 97.3%	
DNS	Densification D_r = 91%, D_c = 105.6%	2
P4D	Log piling, Interval = 4D a_s = 4.9%, D_r = 70% D_{ro} = 54%, D_c = 99.1%	

D: Diameter of the log at the top
a_s: Improvement ratio
D_r: Relative density of ground between the log piles
D_{ro}: Initial relative density
D_c : Degree of compaction (%)

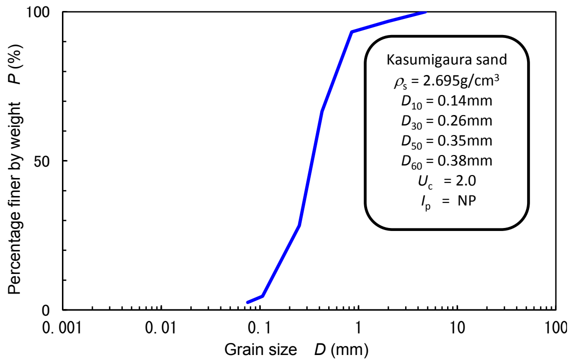

Fig.1. Particle size distribution curve for sand sample.

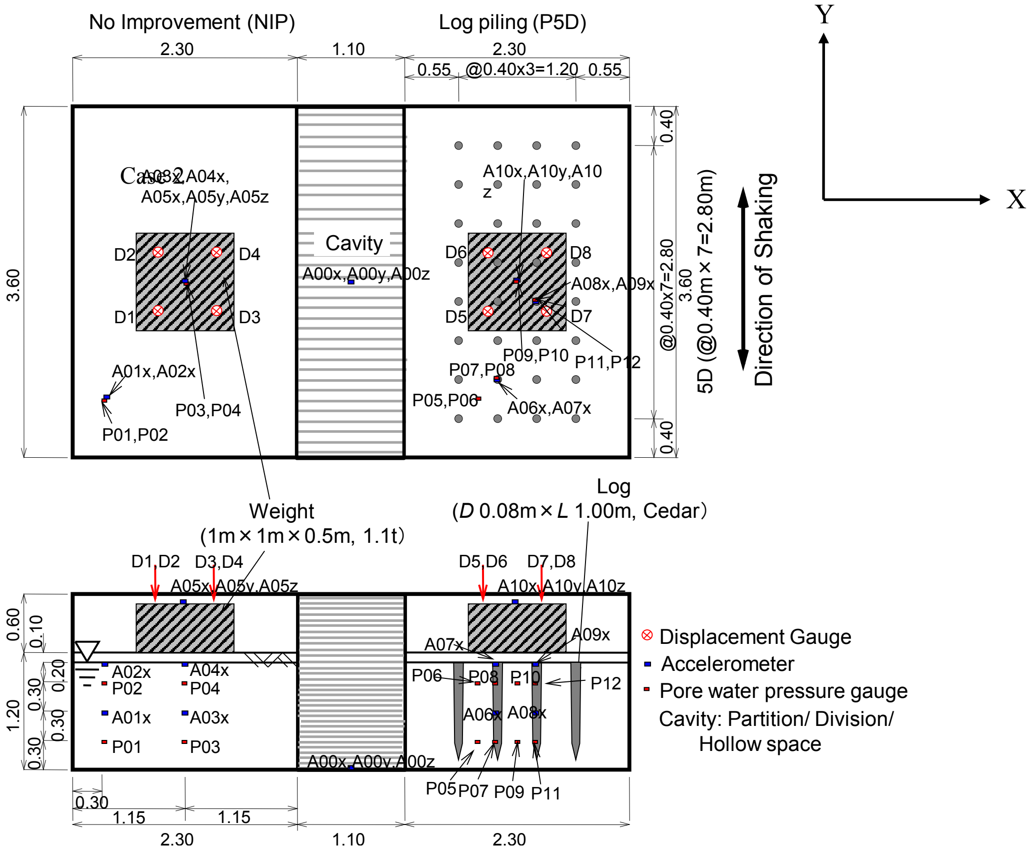

(a) NIP & P5D

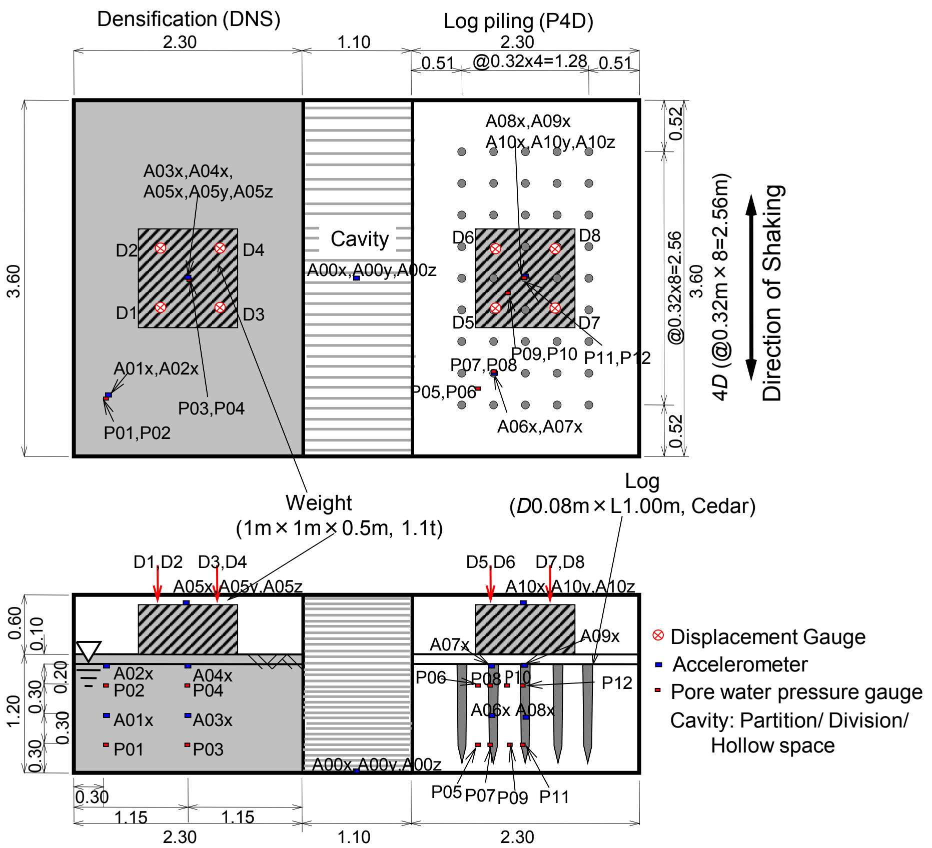

(b) DNS & P4D

Fig.2 Sensor location in large-scale shaking table test.

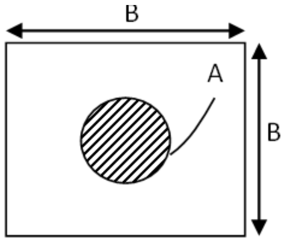

Fig.3 Improvement ratio.

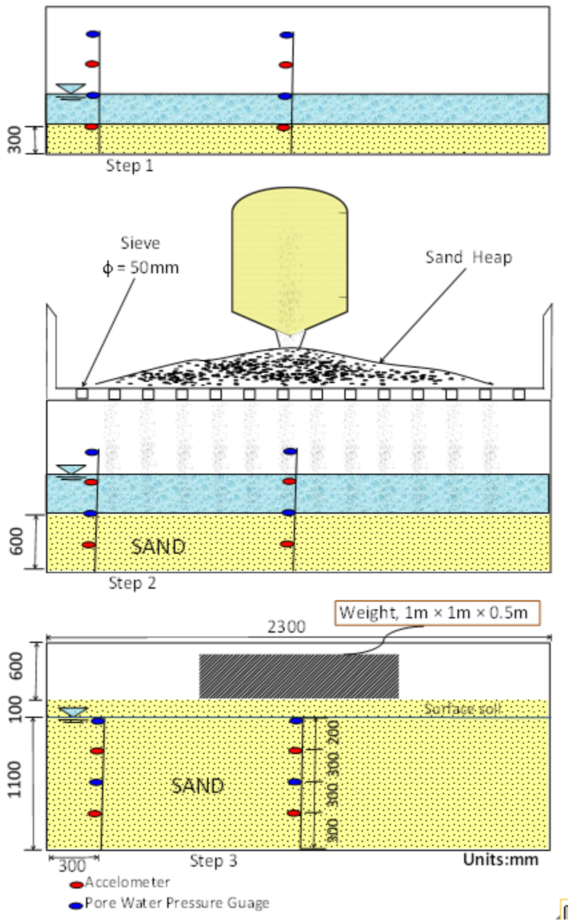

Fig.4 (a) Schematic of unimproved model ground.

The initial relative density D_{ro}, the relative density after improvement D_r, and the improvement ratio are shown in **Table 1**.

The improvement ratio a_s is defined as the percentage improvement of the improved foundation over its unimproved state, which is calculated by the interval between the logs (4*D*, 5*D*) and the cross section of the log at the top as follows (shown in **Fig. 3**):

$$a_s = \frac{A}{B^2} \tag{1}$$

In the log piling method, the relative density D_r was calculated by the density between the log piles using the diameter at the top of the log piles multiplied by the ground thickness. In the densification method, the relative density D_r was calculated by the ground thickness.

(5) Model ground construction

a) Natural model ground (NIP)

The natural model ground was constructed using the following procedure and as shown in **Fig. 4 (a)**:

1) Sensors were installed at each layer level, i.e., heights of 300, 600, 900, and 1,100 mm.
2) Wet sand was poured through a perforated mesh into the water to a maximum thickness of 300 mm.
3) This procedure was done twice to make sand layers reach heights of 600 mm and 1,100 mm. After each layer was created, the ground was leveled.
4) Water level was set at a height of 1,000 mm.
5) A layer of surface soil with a thickness of 100 mm was placed on the ground and the ground was leveled. This step completed the initial construction of the ground.

b) Compacted model ground (DNS)

The compacted model ground was constructed as follows:

1) Sensors were installed at the same depth as the initial ground.
2) Wet sand was poured into the water to achieve a maximum thickness of 300 mm.
3) The soil was compacted with a vibrator to check the density of the soil.
4) This procedure was done twice to construct sand layers with heights of 600 mm and 1,100 mm. After each layer was created, the ground was leveled.
5) The water level was established at a height of 1,000 mm.
6) Surface soil with a thickness of 100 mm was placed on the ground and then the ground was leveled. This step completed the construction of the compacted model ground.

c) Log piling model ground (P5D, P4D)

The log piling ground was constructed as follows and as shown in **Fig. 4 (b)**:

1) The initial ground was constructed using the same steps for the NIP model ground.
2) Piles were statically pushed into the ground at pre-determined intervals and alternate positions.
3) Piles were inserted into the ground between the previously inserted piles.
4) After installing the piles, drains were placed above the heads of the piles at a depth of 10 cm. Weight was placed on the surface of the ground after completion of the model ground.

(6) Input motion

The model ground was shaken in a horizontal direction with a sinusoidal wave with peak amplitude of 50 Gal, frequency of 4 Hz and duration of 8 sec, as shown in **Fig. 5**. The pore water pressures and response accelerations were simultaneously recorded

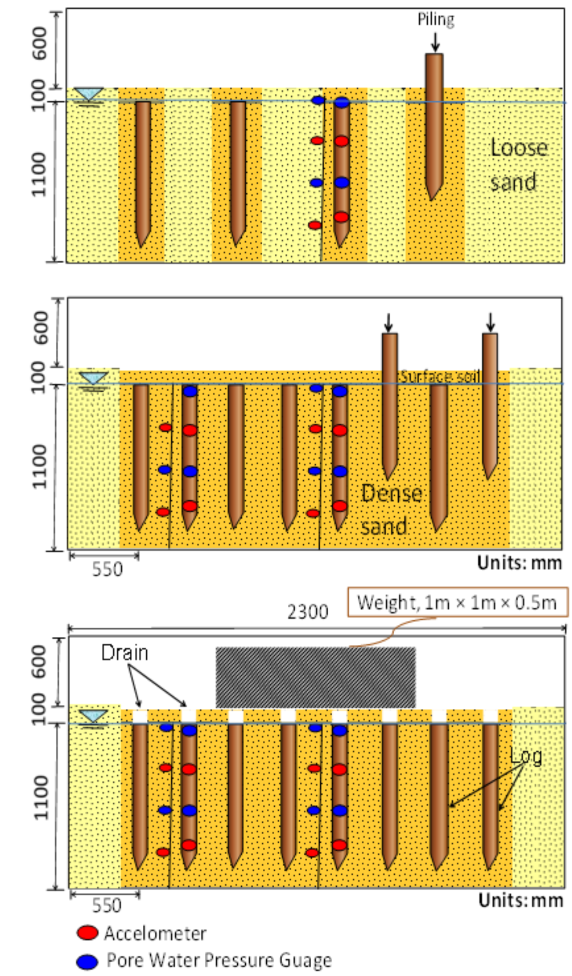

Fig.4 (b) Model ground preparation for P5D.

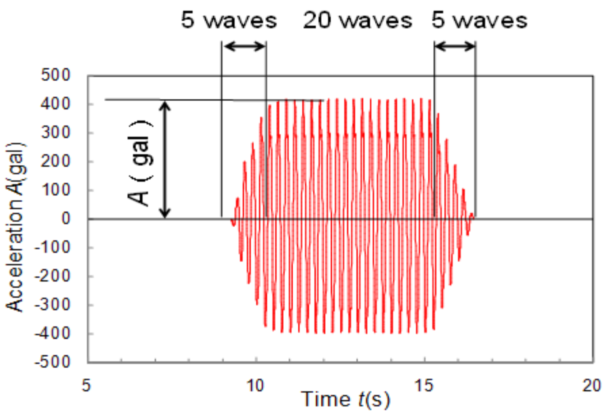

Fig.5 Input motion of large scale shaking table.

on the data recorder. After the excess pore water pressure had completely dissipated, the vertical displacements of the logs and the ground surface were measured by a point gauge.

Constant amplitude of twenty cycles was recorded with five waves increasing at the beginning and five waves decreasing at the end. The process was repeated eight times with different amplitudes, which ranged from 50-400 Gal with an interval of 50 Gal.

3. RESULTS OF SHAKING TABLE TEST

(1) Time history during shaking

Fig. 6 shows an example of the acceleration time history with the same target input acceleration of 150 Gal. The value σ_{v0}' is the initial effective overburden pressure that was calculated from the density, as mentioned in **Fig. 6**. An equivalent input acceleration yields a different structural response when logs are used.

The unimproved ground experiences a large settlement, whereas the settlement decreases and is almost negligible in the log piling method. In the case of NIP, the settlement of the structure began when the pore water pressure achieved an initial effective overburden pressure at P02, but the increase in pore water pressure for P4D was not significant. This performance is almost identical to the performance for DNS; however, in the case of P5D, the performance of shaking table varies between the performances of NIP and P4D. Therefore, the pore water pressure substantially influences the settlement of the structure.

In the case of NIP, the response acceleration at A02 and A05 differs despite an equivalent relative density and input acceleration, which may be attributed to the overburden pressure condition. A05 was mounted on the model structure and A02 was buried inside the ground. The response accelerations at A05 and A10 differ, which may cause a significant shear stress under the weight.

(2) Settlement of model structure and excess pore water pressure

Fig. 7 shows the relationship between the excess pore water pressure ratio and the settlement under the weight. The excess pore water pressure ratio is calculated as the excess pore water pressure divided by the effective overburden pressure ($\Delta u/\sigma_v'$). Large settlement occurred when an excess pore water pressure of approximately 1.0 was achieved. It is the point where the increase in pore water pressure (Δu) is equivalent to the initial vertical effective overburden stress ($\Delta u/\sigma_{vo}'$=1.0). The water pressure becomes sufficiently high to counteract the gravitational pull on the soil particles and effectively 'float' or suspend the soil particles.

The pore water pressure and the settlement of the structure were obtained during the shaking table test. The initial effective overburden pressure was calculated by multiplying the thickness of the sand layer by the unit weight of sand (γH). The excess pore water pressure ratio was calculated by dividing by the effective overburden pressure. An excess pore water pressure of 1.0 corresponds to approximately

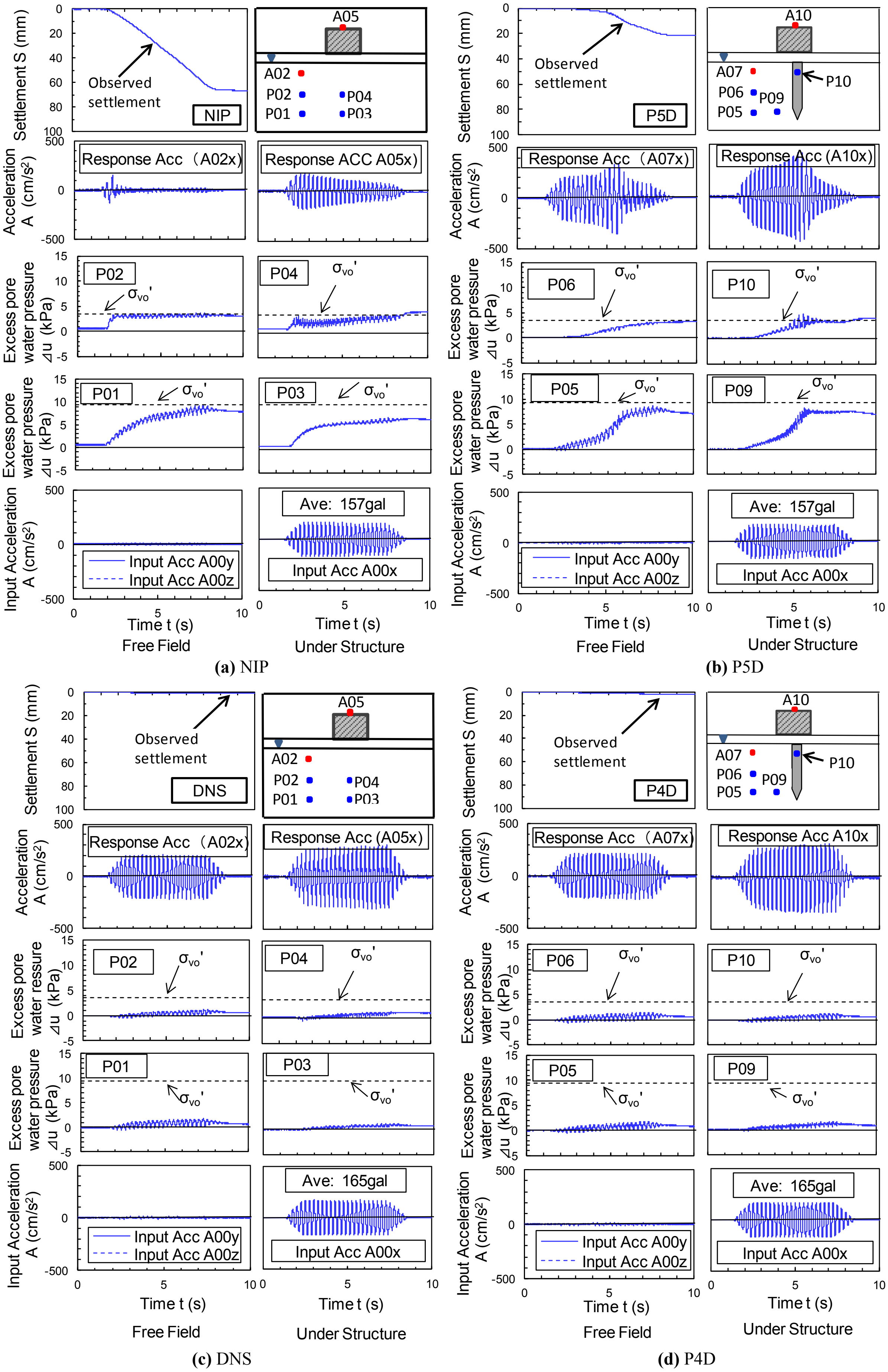

Fig.6 An example of time history of shaking table test (target input motion 150Gal).

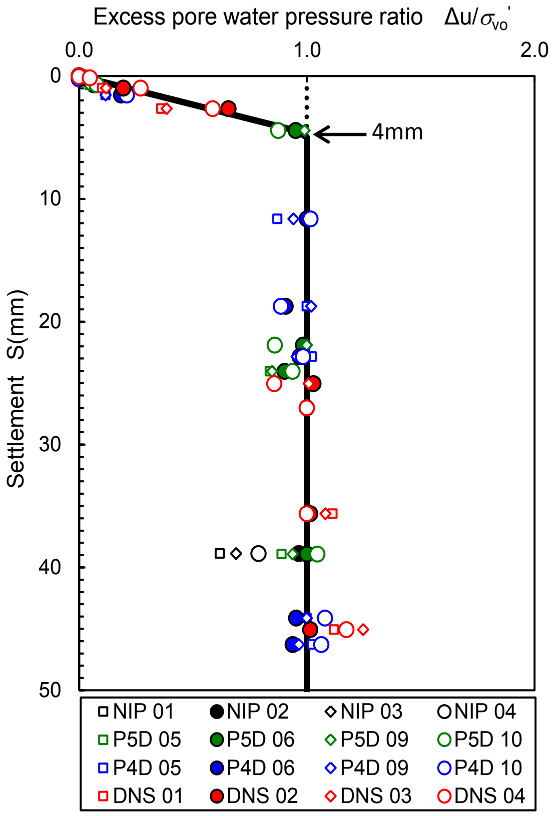

Fig.7 Relationship between excess pore water pressure ratio and settlement.

4 mm of settlement.

Therefore, the point at which a settlement of 4 mm is obtained defines the point that the ground begins to liquefy; the acceleration at this point is defined in this paper as the cyclic resistance.

(3) Input acceleration and cumulative settlement

Fig. 8 shows the relationship between the input acceleration (A_i) and the cumulative amount of settlement based on the results improved by increasing density and log piling. A large settlement of approximately 50 mm occurred for 100 Gal in the case of NIP. For P5D, a small settlement occurred for 150 Gal. In the cases of P4D and DNS, a small settlement occurred for more than 200 Gal.

P4D (D_r = 70%) performed well and similar to the densification method (D_r = 91%). **Fig. 8** shows that the relationship between settlement and relative density is inversely proportional, i.e., the settlement of the soil decreases with increasing relative density. Thus, increasing density can effectively improve a liquefiable ground. Settlement decreases with a decreasing interval of piles.

In **Fig. 8**, the shape of the curve for the log piling method (P4D, P5D) differs from the shape of the curves for NIP and DNS. The curve for log piling is concave down and becomes constant at the end, whereas the DNS curve is similar to the NIP curve, which exhibits a decreasing trend. The curves behave differently, whereas physical parameters such as the shaking table, the container size, the ground water table location, the soil type, and the thickness of the soil are identical in both cases, with the exception of the log piles.

In the case of log piling, the soil assumed the load and resisted against earthquake motion when the model ground was shaken. However, when the input motion was excessive and continually increased, the soil liquefied and the load was transferred to the logs. Because the log cannot liquefy absolutely, the logs are capable of supporting weight if the ground improved by the log piling method experiences unexpected large motion. Therefore, this method is fail-safe against liquefaction damage.

(4) Liquefaction assessment

Fig. 9 shows the relationship between relative density (D_{rmm}) and cyclic resistance, in which D_{rmm} is the relative density calculated by the minimum method[27].

Input motions for four cases are determined for a settlement of 4 mm, as shown in **Fig. 8**. These input accelerations are used as cyclic resistances to assess the liquefaction potential, as shown in **Fig. 9**.

R_{20} is the cyclic resistance ratio at 20 cycles (τ_d/σ_{vo}') where σ_{vo}' is the initial effective overburden pressure and τ_d is the shear stress. In the case of these experiments, the cyclic resistance ratio is the cyclic resistance divided by the acceleration due to gravity (980 Gal).

$$\tau_d = \rho_t h A_i \tag{2a}$$

$$\sigma_{vo}' = \rho_t G h \tag{2b}$$

$$\frac{\tau_d}{\sigma_{vo}'} \approx \frac{A_i}{G} \tag{2c}$$

Because the main input motion consists of 20 waves, this cyclic resistance ratio is nearly equivalent to the cyclic resistance R_{20}, which is defined by elemental tests.

The results for Tonegawa sand determined by the cyclic undrained triaxial test[28] are also plotted in **Fig. 9**. Piles with smaller pile intervals result in greater soil compaction between the piles due to the decreasing volume of the sand ground. The liquefaction resistance of soil increases with increasing soil density. Cyclic resistance for dense specimens with relative densities 91%, 70%, and 64% is increased three times as compared to the no-improvement ground with relative density 48%.

The reason for the R_{20} of Tonegawa being larger than the R_{20} of DNS may be attributed to the finding

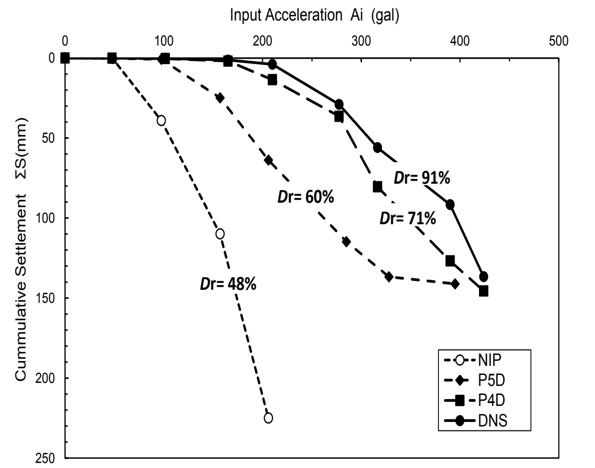

Fig.8 Relationship between input acceleration and cumulative settlement.

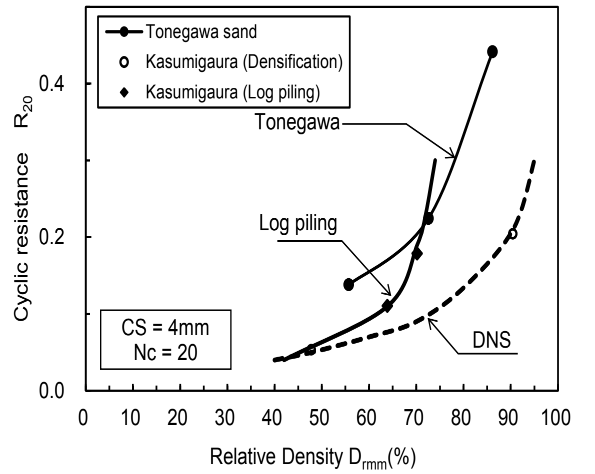

Fig.9 Relationship between relative density and cyclic resistance.

that the response acceleration at the ground surface is larger than the response acceleration of the input motion. If response accelerations are used for DNS, then the DNS curve will be higher and closer to the Tonegawa curve (elemental test line). The R_{20} of the log piling is larger than the R_{20} of the DNS for the same relative density and the same input motion.

(5) Relationship between relative density and settlement

Fig. 10 shows the relationship between relative density and the amount of settlement at the 150 Gal target input acceleration to compare the densification method with the log piling method. **Fig. 10** was developed using the settlement value at 150 Gal from **Fig. 8** for four different cases (NIP, P5D, P4D, and DNS). The relative density in the ground between the log piles was calculated considering the change in ground surface height.

Settlements of the ground that were improved by log piling were less than the settlements obtained by the densification method, which indicate that log piling is more effective than the densification method for the same relative density.

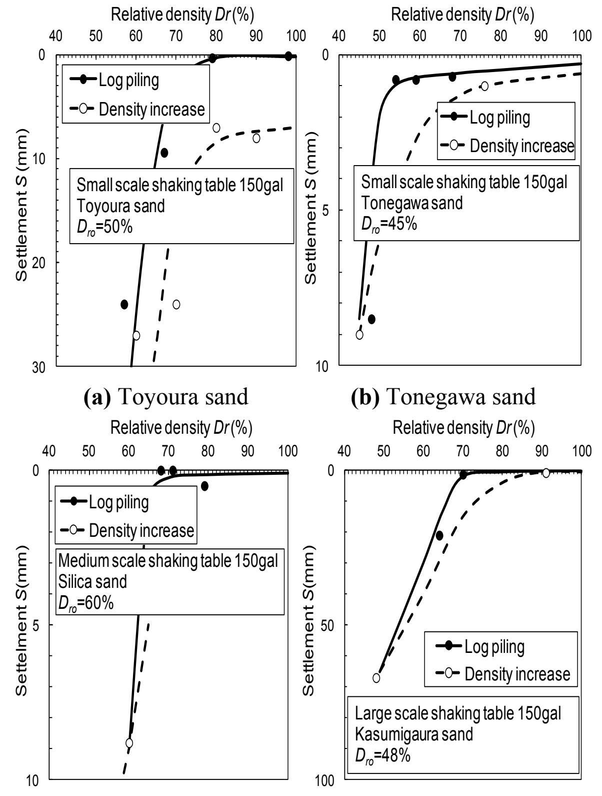

(a) Toyoura sand **(b)** Tonegawa sand

(c) Silica sand **(d)** Kasumigaura sand

Fig.10 Relationship between relative density and settlement.

In **Fig. 10**, four types of sands (Kasumigaura, Silica, Toyoura, and Tonegawa) are used to verify the performance of other sands and the scales of the shaking table. Toyoura sand is a special sand with no fine particles (0%). Silica sand is artificial sand with 11% fine particles, and Tonegawa sand is natural sand with 8% fine particles.

A small-scale container with internal dimensions of 760 mm × 400 mm × 280 mm was used to perform the tests on Toyoura sand and Tonegawa sand. For the small-scale test, an input motion of 5 Hz with 5 waves in the rising part, 22 main motion waves and 5 waves in the ending part was observed. The input motion was uniaxial in the longitudinal direction of the shaking table. The input motion increased the amplitude of this wave at every 50 Gal stage [29]. A weight of 11.5 kg was placed on the model ground to measure the settlement under the weight.

A medium-scale container with dimensions of 1,000 mm × 2,500 mm × 1,000 mm was used to perform tests on the silica sand. An input motion of 1.5 Hz with 22 waves in the rising part, 30 main motion waves and 7 waves in the ending part was observed. In the medium-scale container, no weight was placed on the surface of the model ground and the settlement was determined by measuring the settlement of the ground surface[30].

In each case, the log piling line is always above the density increase line, which indicates that log piling is more effective than the densification method.

4. GROUND INVESTIGATION BETWEEN LOGS

Numerous factors affect liquefaction strength, e.g., relative density, coefficient of cohesion Cc, grain size distribution, soil type, confining pressure, permeability of soil, prior stress-strain history and overconsolidation ratio.

In this paper, the relative density and confining pressure are considered to be the key factors for improving liquefaction resistance. The model grounds were strengthened by the log pile and densification methods.

The ground improved by the DNS method is strengthened by densification. Numerous types of soundings were performed to explain the increase in liquefaction resistance in the case of the ground improved by log piling.

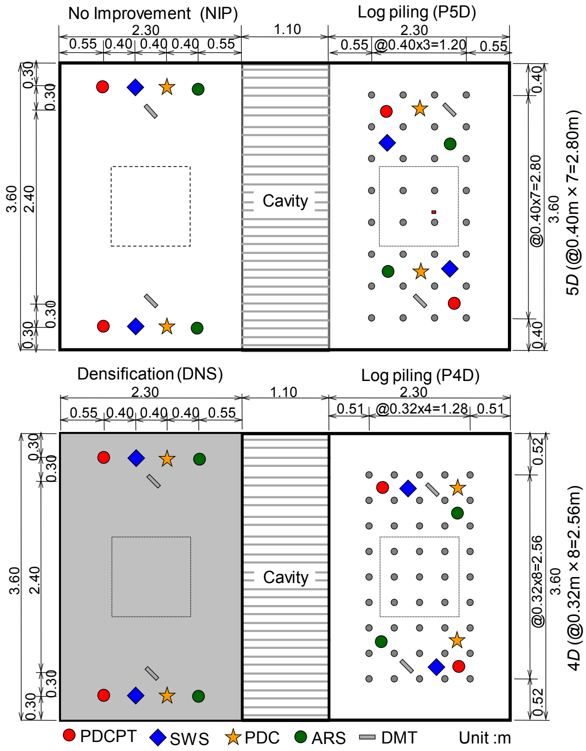

Fig.11 Positions of sounding tests.

(1) Sounding tests

The following tests were performed on the model ground:

a) Portable dynamic cone penetration test (PDCPT)
b) Swedish weight sounding (SWS) test
c) Automatic ram sounding (ARS) test
d) Piezo drive cone (PDC) test

The results of these tests and the flat dilatometer (DMT) test will be separately discussed.

a) Portable dynamic cone penetration test

The PDCPT is performed by dropping a 5 kg hammer from a height of 50 cm to measure the penetration depth per blow for each tested depth[31]. The penetration depth ranges from 100 to 120 cm and the cone diameter is 2.5 cm with a 60° angle with the bottom edge.

The following formulae[32] are used to calculate the corrected N value for *PDCPT*:

If $N_d > 4$

$$N = 1.1 + 0.30N_d \tag{3a}$$

If $N_d \leq 4$

$$N = 0.66N_d \tag{3b}$$

where N_d is the number of blow counts to a maximum depth of 100 mm (number).

b) Swedish weight sounding test

The equipment for this test consists of a screw point at the tip, a steel rod with a length of 1 m, a dead weight of 1,000 N and a top handle. The equipment is rotated and the number of half rotations (180° rotations) required for 1 m of penetration is counted (N_{sw})[33]. If the soil is hard, N_{sw} is significant.

The following formula[34] is used to calculate the N value obtained from the SWS test:

$$N = 0.002W_{sw} + 0.067N_{sw} \tag{4}$$

where
W_{sw}: dead weight of Swedish sounding (N)
N_{sw}: number of half rotations (180° rotations) for a 1 m penetration.

c) Automatic ram sounding test

In the automatic ram sounding test, a rod with a length of 1 m, a diameter of 32 mm and a weight of 63.5 kg is used. The cone has an outside diameter of 45 mm, length of 90 mm and weight of 5 kg. The height of fall for the ARS is 500 mm and the depth of penetration is 200 mm[35].

For ARS

$$N = N_d \tag{5a}$$

If $N_d \leq 5$

$$N_d = N_{dm} \tag{5b}$$

If $N_d > 5$

$$N_d = N_{dm} - \Delta N_{dm} \tag{5c}$$

where
N_d: number of blow counts (number)
N_{dm}: mean number of blow counts to a maximum

depth of 200 mm (number)
ΔN_{dm}: mean number of blow counts due to friction or torque (number).

d) Piezo drive cone test

The PDC is a handheld device designed to penetrate soils to depths of 1 m with a 20 mm diameter cone.

The 60° cone is forced into the ground by rising and dropping an 8 kg hammer[36]. The following formulae[37] are used to calculate the corrected N value for the PDC:

$$N_d = \frac{1}{2} N_{dm} \tag{6a}$$

$$N \approx N_d$$

$$N_d = \frac{10}{d} - 0.16 M_r \tag{6b}$$

where
N_{dm}: mean value of blow counts to a maximum depth of 20 cm
N_d: penetration resistance
d: penetration depth (cm)
M_r: torque or moment (N-m).

(2) Results of sounding tests

Fig. 11 shows the positions of the sounding tests performed before and after the improvement in the ground. **Fig. 12** shows the results of the sounding tests, which show the relationship between the SPT N-value and the depth.

The SPT N-values explained in the figures were obtained from each sounding test and converted from each result. The data for equivalent depths were averaged for each case. The results of the NIP case by ARS was almost zero because the blow energy was too strong for very loose sand.

The results show that the N-value increases with increasing depth; the N-values of P5D, P4D, and DNS are greater than the N-values of NIP; and the N-values of P4D are greater than the N-values of P5D, with the exception of PDCP and ARS. The increase in the N-value with increasing depth can be attributed to the increase in confining pressure and improved density. Due to the increase in the N-value, the density of the ground also increases. These results reveal that the ground between the logs was strengthened by log piling and the densification method.

Fig. 13 shows the relationship between the relative density and the N-values for a depth of 0.7 m. The relationship obtained by Meyerhof[38] is also plotted in **Fig. 13**. Meyerhof's data significantly differ from the data in this paper. Because the overburden pressure in this study is considerably low, the absolute value is not important; however, the shape is useful information.

DNS is only one datum; thus, the relationship obtained by the densification method was denoted by a broken red line, which signifies Meyerhof's relationship. The relationship obtained by log piling yields a higher N-value than the relationship obtained by the densification method. Due to an increase in the N-value for the ground between the piled logs, the density of the ground also improved.

(3) Flat dilatometer test

Confining pressure is one of the most important factors affecting liquefaction resistance. DMT was used to estimate the lateral stiffness or horizontal earth pressure of the soil before and after improvement by DNS and log piling.

The flat dilatometer is an in situ device that is used to determine the in situ soil lateral stress and the soil lateral stiffness, and to estimate other engineering properties of subsurface soils. This test measures the horizontal earth pressure by placing a board-shaped instrument with a thickness of 15 mm and a width of 96 mm width into the ground and pushing the ground horizontally using a circular expandable steel membrane with a diameter of 60 mm on one side.

The test involves driving this steel blade into the ground, inflating the steel membrane and measuring the corresponding pressure and deformation. The penetration of the steel blade is usually achieved using common in situ penetration equipment; for instance, the equipment used in the standard penetration test. The DMT can be used to test extremely soft soils to extremely stiff soils[39].

The primary reason for the increased N-value for the ground between the piled logs is the increased density and confining pressure. To clarify the effect of confining pressure, the horizontal earth pressure was measured by the DMT. The horizontal earth pressure was measured at two points for each case of NIP, P5D, P4D, and DNS. The data from the NIP were used as the original ground data prior to improvement.

Fig. 14 displays the results of the DMT: (a) shows the effective horizontal earth pressure with depth and (b) shows the rate of increase after improvement. The data obtained from the two points in each case were averaged at the same depth. No datum is obtained using the DMT for depths greater than 0.5 m because the NIP ground was too soft for this instrument. The rates of increase exceed 1.0 and range from approximately 1.1 to 1.5, with the exception of one point. The horizontal earth pressure increases from 1.1 to 1.5 times as large as the pressure prior to improvement. The increase in the N-value may be due to the increasing horizontal earth pressure.

(4) Verification of remedial measures

The reduction in the susceptibility to liquefaction is

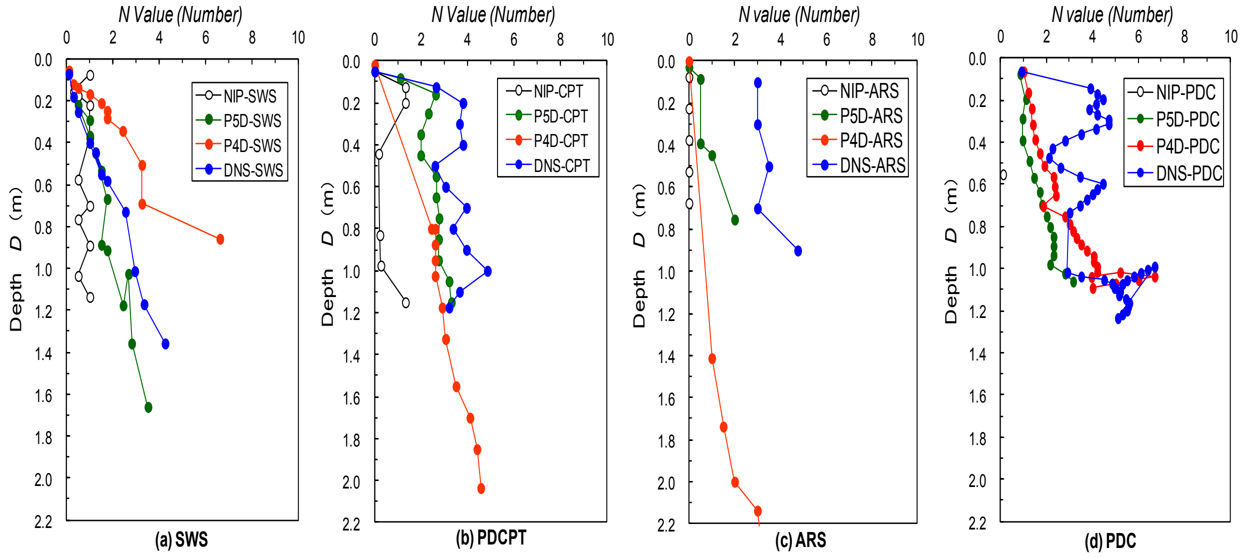

Fig.12 Results from the sounding tests.

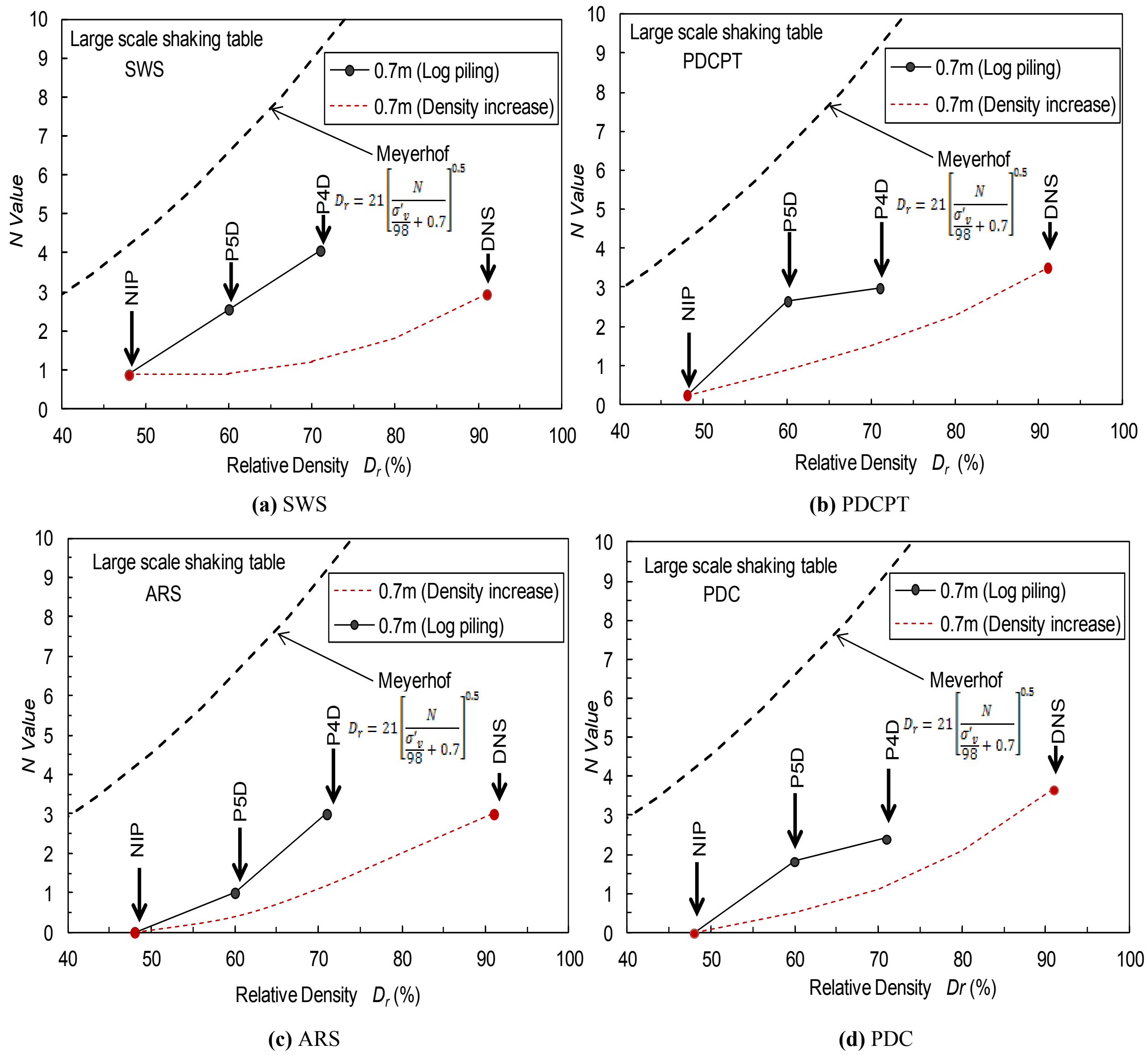

Fig.13 Relationship between relative density and N values.

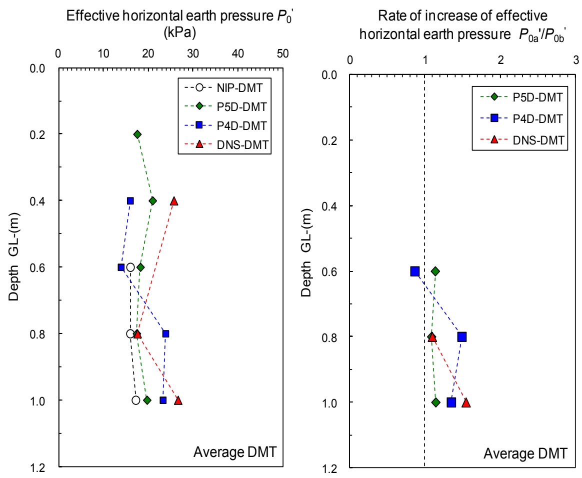

Fig.14 Results of the DMT.

based on the increase in *N*-values (strength) and confining pressure. Because no direct method can be used to estimate the increased liquefaction resistance, the effect of ground improvement (degree of compaction) was confirmed by *N*-values obtained from different sounding tests.

Another reason for the increased liquefaction resistance is that the shear modulus of the ground-logs complex ground is higher than the shear modulus of the original ground. The shear modulus of wood is approximately 600 MPa and the shear modulus of the ground is approximately 10 MPa. Therefore, the shear modulus of the combined ground-logs composite ground is higher than the shear modulus (610 MPa) of the original ground. The liquefaction resistance is higher due to the increase in the shear modulus of the improved ground. Sounding tests (SWS, PDCP, ARS, and PDC) and flat dilatometer tests were used to confirm the effective improvement on liquefaction.

Another reason for the reduced liquefaction may be the dissipation of pore water pressure along the periphery of the logs. During driving, the shear stress along the direction of the axis of the pile caused an increase in the total radial stress, which in turn caused an increase in the pore water pressure. The excess pore pressures generated in this process are subsequently assumed to dissipate by outward radial flow of pore water along the surface of the pile. Thus, the ground will densify due to the increase in effective radial stress.

In addition, it is easy to generate a void and water film between the surface of the wood and the particles of sand because the surface of the wood is coarse and wooden piles move laterally by shaking. Therefore, water can dissipate along the periphery of the logs. As a result, resistance to liquefaction should increase.

5. CONCLUSIONS

A series of 1g shaking table tests was carried out to evaluate the performance of two ground improvement techniques against liquefaction, log piling, and densification. A test with no improvement was also performed to compare the behaviors of sands.

Considering the effect of installing log piles in densifying the ground and densification by compacting the soil, liquefaction analysis is proposed that uses pore pressure generation and settlement of structure for the ground treated with log piles. Both the settlement of structure and excess pore water pressure are considered to be affected as they decrease because of densification. This densification decreases with distance from the log pile. Observing the test macroscopic phenomenon and analyzing the data of pore pressure and settlement, the following conclusions were reached:

1) The effect of liquefaction mitigation by the log piling method is larger than the effect of liquefaction mitigation by the densification method.
2) The degree of compaction is increased by 106% by the log piling method and 113% by the densification method as compared to unimproved ground.
3) If the ground improved by the log piling method experiences significant earthquake motion, the log is capable of supporting overburden stress because the log cannot liquefy absolutely. Therefore, this method is fail-safe against liquefaction damage.
4) The effect of liquefaction mitigation by the log piling method increases with decreasing intervals between the logs and by piling logs with 4*D* intervals, which is equivalent to the effect of the densification method with 91% relative density.
5) The primary reason for the increase in liquefaction resistance is that the ground is strengthened by an increase in density and confining pressure.
6) Results of tests performed on loose specimens (D_r=48%) indicate that higher pore pressure is developed with decreasing relative density. Loose specimens showed up to three times higher liquefaction potential compared to dense specimens (D_r=91%, 70%, 64%).
7) Safe side design for log piling method is possible for liquefaction mitigation by estimating liquefaction resistance from calculated ground density between log piles.
8) Ground-logs complex ground has higher shear modulus than original ground; therefore, liquefaction resistance will also increase.

ACKNOWLEDGEMENTS: The financial assistance provided by Waseda University, Japan is gratefully acknowledged. The authors acknowledge Professor Masanori Hamada (Waseda University) for his continued support. The authors are grateful for the assistance of Masaho Yoshida (Professor), Takumi Murata (Fukui National College of Technology), Tadashi Hara (Associate Prof.), Akiko Sakabe (Kochi University) and Syusei Ogawa (Nagaoka University of Technology) in the shaking table tests. The authors also appreciate the assistance by the staff members of Tobishima Corporation, especially Shigero Miwa.

REFERENCES

1) Tokimatsu, K. and Katsumata, K.: Liquefaction-induced damage to buildings In Urayasu city during the 2011 Tohoku Pacific Earthquake, *Proceedings of the International Symposium on Engineering Lessons Learned from the 2011 Great East Japan Earthquake*, Tokyo, Japan, 2012.
2) Yoshida, M., Miyajima, M. and Numata, A.: Experimental Study on liquefaction countermeasure technique by log Piling for residential houses, *15th World Conference on earthquake Engineering (15th WCEE)*, Lisbon, Portugal, 2012.
3) Orense, R.P.: Soil liquefaction and slope failures during the 2011 Tohoku, Japan Earthquake, *NZSEE Annual Technical Conference & AGM*, 2012.
4) Ochi, S. and Suzuoki, M.: The lessons of the Great East Japan Earthquake 2011 and the countermeasures against earthquakes and tsunami in future- Fundamental Concepts behind Future Tsunami Disaster Prevention, *Proceedings of the 43rd joint meeting of U.S.-JAPAN panel on wind and seismic effects*, UJNR, pp. 49-60, 2011.
5) Finn, W.D.L., Pickering, D.J. and Bransby, P.L.: Sand liquefaction in triaxial and simple shear tests, *Journal of Soil Mechanics and Foundations Division*, ASCE 97 (SM4), pp. 639-659, 1971.
6) Idriss, I.M. and Boulanger, R.W.: Semi-empirical procedures for evaluating liquefaction during earthquakes, *Journal of Soil Dynamics and Earthquake Engineering,* Vol. 26, pp. 115-130, 2006.
7) Ishihara, K.: Liquefaction and flow failure during earthquakes, *Geotechnique,* Vol. 43, No. 3, pp. 321-376, 1993.
8) Ishihara, K. and Yoshimine, M.: Evaluation of settlements in sands deposits following liquefaction during earthquakes, *Soils and Foundations,* Vol. 32, No. 10, pp. 173-188, 1992.
9) Seed, H. B. and Idriss, I. M.: Evaluation of liquefaction potential of sand deposits based on observations of performance in previous earthquakes, *In-situ Testing to Evaluate Liquefaction Susceptibility, ASCE National Convention*, St. Louis, Missouri, pp. 81-544, 1981.
10) Ueng, T. S.: Shaking Table Tests for Studies of Soil Liquefaction and Soil-Pile Interaction, *Geotechnical Engineering Journal of the SEAGS & AGSSEA*, Vol. 41, No.1, pp. 1-10, 2010.
11) Towhata, I.: *Geotechnical Earthquake Engineering*, Springer Series in Geomechanics and Geoeng*ineering, 2008.*
12) Hamada, M. and Wakamatsu, K.: Liquefaction, Ground Deformation and their caused damage to structures, *The 1995 Hyogoken-Nanbu earthquake - investigation into damage to civil engineering structures*, *Committee of Earthquake Engineering,* Japan Society of Civil Engineers, pp. 45-92, 1996.
13) Yoshimi, Y. and Tokimatsu, K.: Settlement of buildings on saturated sand during earthquakes, *Soils and Foundations*, Vol. 17, No. 1, pp. 23-38, 1977.
14) Tokimatsu, K.: Recommendations for design of building foundations considering liquefaction and lateral spreading, *The Kenchiku Gijutsu*, No. 563, pp. 126-131, 1997. (in Japanese)
15) Idriss, I. M. and Boulanger, R. W.: *Soil Liquefaction During Earthquakes*, Earthquake Engineering Research Institute (EERI), 2008.
16) Yoshida, N., Yasuda, S., Kiku, M., Masuda, T. and Finn, W. D. L.: Behavior of sand after liquefaction, *Proceedings of 5th US-Japan Workshop on Earthquake Resistant Design of Lifeline and Countermeasures against Soil Liquefaction*, pp. 181-198, 1994.
17) Yasuda, S. and Ogasawara, M.: Studies on several countermeasures against liquefaction-induced flow and an application of a measure to existing bridges in Tokyo, *Journal of Japan Association for Earthquake Engineering (JAEE),* Vol.4,No.3(Special Issue), pp. 370-376, 2004.
18) Numata, A., Yoshida, M. and Hamada, M.: An example of applying wood piles as a countermeasure against liquefaction during the 1964 Niigata earthquake, *Journal of Japan Wood Research Society (JWRS*), ISSN:0021-4795, Vol.55, No.5, pp. 305-315, 2009.
19) Yoshida, M., Miyajima, M. and Numata, A.: Liquefaction Countermeasure Technique by Using Logs, *Progress of Geo-Disaster Mitigation Technology in Asia,* Springer, pp. 293-311, 2012.
20) Metz, B., Davidson, O. R., Bosch, P. R., Dave, R., Meyer, L. A. (eds) : Contribution of Working Group III to the Fourth Assessment Report of the Intergovernmental Panel on Climate Change, IPCC, pp. 27-93, 2007.
21) Report on Research and Development in Agriculture, Forestry and Fisheries No.23, Impact of Global Warming on Agriculture, Forestry and Fisheries and Possible Countermeasures in Japan, Agriculture, Forestry and Fisheries Research Council, Ministry of Agriculture, Forestry and Fisheries, Japan, 2007.
22) Ramanathan, V. and Carmichael, G.: Global and regional climate changes due to black carbon, *Nature Geoscience,* Vol. 1, pp. 221–227, 2008.
23) Muschett, F.D.: Integrating Global Sustainable Development and Environmental Conservation, *Next Generation Climate Mitigation*, pp.18-21, 2004.
24) Richard, S.L.: On the scientific basis for global warming scenarios, *Environmental Pollution,* Vol. 83, pp. 124-134, 1994.
25) Numata, A., Motoyama, H., Momohara, I., Nagao, H., Hamada, M. and Yoshida, M.: Method of small-scale shaking table test on measures against liquefaction by tree trunks piling, *Proceedings of the 13th International Summer Symposium in conjunction with JSCE 66th Annual Conference,* Japan Society of Civil Engineers, CS13, pp. 17-18, 2011. (in Japanese)
26) Kishida, K., Tsutsumi, K., Nakamati, R., Tonsho, N. and Hamada, M.: An experimental study on measures by wooden pile foundations against soil liquefaction and ground flow, *Proceedings of the 10th Symposium on the Use of Wood for Civil Engineering*, Japan Society of Civil Engineers, pp. 95-101, 2011. (in Japanese)
27) Numata, A. and Shimamoto, E.: Liquefaction resistance of non-plastic fine soils under condition of SPT N-values and relative density, *Journal of JSCE*, No.764/III-67, pp. 287-305, 2004. (in Japanese)
28) Numata, A. and Shimamoto, E.: Liquefaction resistance of non-plastic fine soils under condition of SPT N-values and

relative density, Journal of JSCE, No.764/III-67, pp. 287-305, 2004. (in Japanese)

29) Riaz, S., Hamada, M., Numata, A. and Motoyama, H.: Development of a countermeasure against soil liquefaction by driving wooden piles, *Proceedings of the 14th International Summer Symposium in conjunction with JSCE 67th Annual Conference,* Japan Society of Civil Engineers, 2012.
30) Riaz, S., Numata, A. and Hamada, M.: Study of liquefaction measures by wooden piles comparing different types of soils, *Proceedings of the 11th Symposium on the Use of Wood for Civil Engineering*, Japan Society of Civil Engineers, pp. 81-86, 2012.
31) Jeffrey, E. H. and Tim, L. J.: A dynamic cone penetrometer for measuring soil penetration resistance, *America Journal of Soil Science Society*, Vol. 66, No. 4, pp. 1320-1324, 2002.
32) Japanese Geotechnical Society: Method for Portable dynamic cone penetration test, *Japanese Standards for Geotechnical and Geo-environmental Investigation Methods*, pp. 274-279, 2004.
33) Tsukamoto, Y., Ishihara, K. and Sawada, S.: Correlation between penetration resistance of Swedish weight sounding tests and SPT blow counts in sandy soils, *Soils and Foundations*, pp. 13-24, 2006.
34) Japanese Geotechnical Society: Method for Swedish Weight Sounding test, *Japanese Standards for Geotechnical and Geo-environmental Investigation Methods*, pp. 280-289, 2004.
35) Japanese Geotechnical Socie*ty: Method for Automatic Ram Sounding test, Japanese Standards for Geotechnical and Geo-environmental Investigation Methods*, pp. 330-331, 2004.
36) ASTM D5778-95: Standard Test Method for Performing Electronic Friction Cone and Piezocone Penetration testing of Soils, ASTM Section 4, Vol. 4.09, *Soil and Rock(II)*, 1997.
37) Sawada, S.: Estimation of liquefaction potential using dynamic penetration with pore pressure transducer, *Proceedings of International Conference on Cyclic Behavior of Soils and Liquefaction Phenomenon*, Bochum, pp. 305-312, 2004.
38) Meyerhof, G.G.: Discussion on soil properties and their measurement, session 2, *Proceedings of 4th International Conference on Soil Mechanics and Foundation Engineering (ICSMFE)*, Vol. III, London, United Kingdom, p. 110, 1957.
39) Marchetti, S., Monaco, P., Totani, G. and Calabrese, M.: The flat dilatometer test (DMT) in soil Investigations, *International Conference on In situ Measurement of Soil Properties*, Bali, Indonesia, 2001.

(Received July 16, 2013)